batteries

MDPI

*Review*

# Research Trends on the Dispersibility of Carbon Nanotube Suspension with Surfactants in Their Application as Electrodes of Batteries: A Mini-Review

**Hyungsub Yoon [1], Haeji Kim [1], Paolo Matteini [2] and Byungil Hwang [1,*]**

[1] School of Integrative Engineering, Chung-Ang University, Seoul 06974, Republic of Korea
[2] Institute of Applied Physics "Nello Carrara", National Research Council, 50019 Florence, Italy
* Correspondence: bihwang@cau.ac.kr

**Abstract:** In the battery field, carbon nanotubes (CNTs) attract much attention due to their potential as a supporting conducting material for anodes or cathodes. The performance of cathodes or anodes can be optimized by introducing densely packed CNTs, which can be achieved with high dispersibility. The efficiency of CNT usage can be maximized by enhancing their dispersibility. An effective technique to this end is to incorporate surfactants on the surface of CNTs. The surfactant produces a surface charge that can increase the zeta potential of CNTs, thereby preventing their agglomeration. Additionally, surfactants having long chains of tail groups can increase the steric hindrance, which also enhances the dispersibility. Notably, the dispersibility of CNTs depends on the type of surfactant. Therefore, the results of dispersibility studies of CNTs involving different surfactants must be comprehensively reviewed to enhance the understanding of the effects of different surfactants on dispersibility. Consequently, this paper discusses the effect of different types of surfactants on the dispersibility of CNTs and presents several perspectives for future research on dispersibility enhancement.

**Keywords:** carbon nanotubes; dispersibility; sedimentation; agglomeration; packing



**Citation:** Yoon, H.; Kim, H.; Matteini, P.; Hwang, B. Research Trends on the Dispersibility of Carbon Nanotube Suspension with Surfactants in Their Application as Electrodes of Batteries: A Mini-Review. *Batteries* **2022**, *8*, 254. https://doi.org/10.3390/batteries8120254

Academic Editors: Mingsheng Wang and Claudio Gerbaldi

Received: 5 October 2022
Accepted: 17 November 2022
Published: 23 November 2022



## 1. Introduction

Single-walled (SWCNTs) or multi-walled carbon nanotubes (MWCNTs) have attracted considerable attention as supporting conducting materials for the cathodes or anodes of batteries owing to their outstanding mechanical and electrical properties (Figure 1) [1–19]. The density of carbon nanotubes (CNTs) considerably influences the performance of the cathode or anode, with a higher density corresponding to superior battery efficiency [20–24]. To achieve a high density of CNTs in a limited volume, CNTs must be dispersed in a processing solvent without severe agglomeration or aggregation [25–30]. To this end, the attraction force induced among the individual CNTs in a solvent must be reduced. The most widely used approach to enhance the dispersibility of CNTs is to use surfactants, which are cost effective and can be easily processed through simple mixing processes such as sonication or mechanical stirring [31–46]. Surfactants incorporated on the CNT surface generate a surface charge (Figure 2) [47]. Anionic or cationic surfactants wrapping the CNT surface are expected to induce negative or positive charges, respectively, thereby increasing the absolute value of the zeta potential measured through an electrophoretic method. A high absolute value of the zeta potential results in a high repulsive force among the CNTs, thereby preventing the agglomeration or aggregation of CNTs. Additionally, surfactants with long chain lengths can enhance the dispersibility by increasing the steric hindrance (Figure 2) [47].

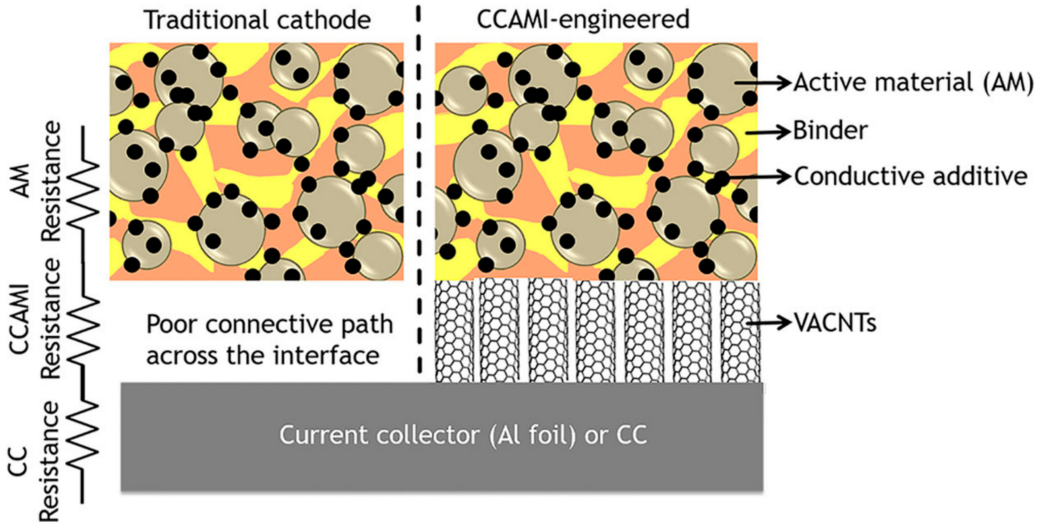


**Figure 1.** Schematic showing various resistances in LIB cathodes. The overall cathode resistance is the sum of the resistances arising from the (1) active material, binder, and conductive additive coatings, (2) CCAMI, and (3) current collector. As shown on the left, in a traditional cathode, conductive additives decrease the electrical resistance within the active material but do not affect the high CCAMI resistance. On the other hand, as shown on the right, VACNTs directly grown on an Al foil enable better electrical conduction across CCAMI, which dramatically improves the LIB performance [3]. Reproduced with permission [3] (American Chemical Society, 2018).

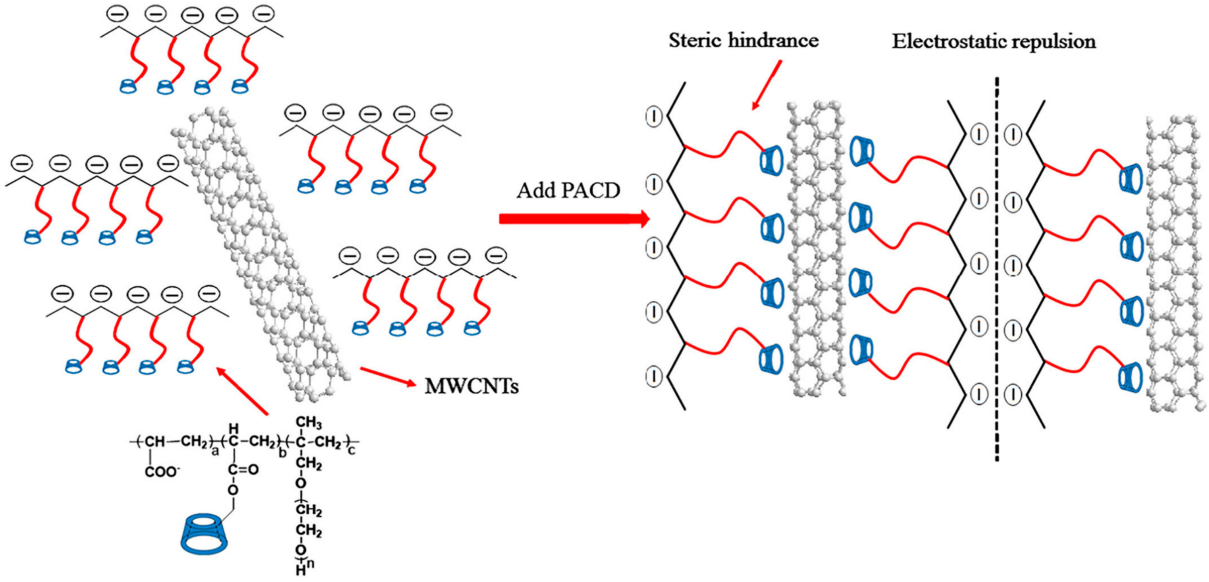


**Figure 2.** Schematic of mechanism of steric hindrance and electrostatic repulsion [47]. Reproduced with permission [47] (John Wiley and Sons, 2018).

Different types of surfactants, such as anionic, cationic, or non-ionic surfactants, have been used to improve the dispersibility of CNTs (Figure 3) [48]. In general, the dispersibility of CNTs in an aqueous solution depends significantly on the type of surfactants. Therefore, it is important to organize the results of various studies on the dispersibility of CNTs involving different surfactants to comprehensively understand the behaviors of CNTs with different surfactants in the dispersion states. This paper summarizes and discusses representative results on the dispersibility of CNTs with different surfactants. Moreover, several perspectives for future research on enhancing the dispersibility of CNTs are presented. The findings can provide a basis for research on enhancing the dispersibility of CNTs using surfactants.

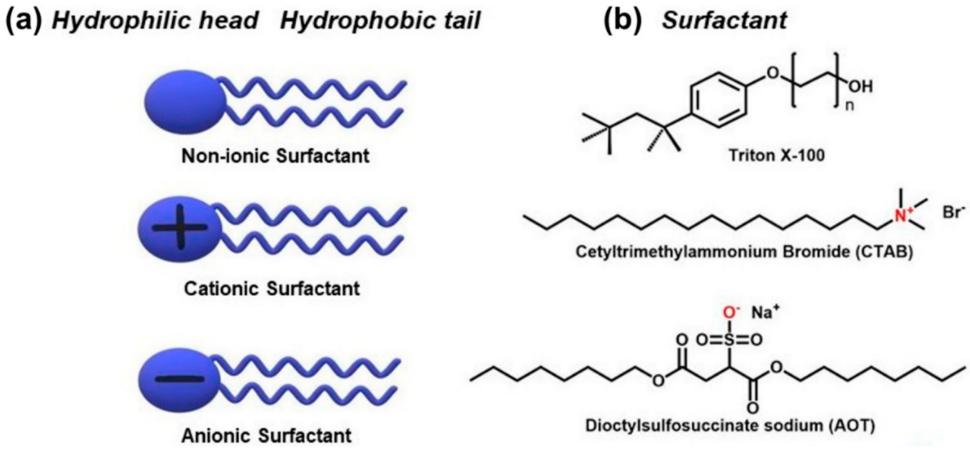


**Figure 3.** (**a**) A schematic of different types of surfactants and (**b**) chemical structures of some common surfactants [48]. Reproduced with permission [48] (MDPI, 2019).

## 2. Enhancing the Dispersibility of CNTs Using Various Types of Surfactants

Jiang et al. used sodium dodecyl sulfate (SDS) as a surfactant to enhance the dispersibility of CNTs [49]. SDS is an anionic surfactant consisting of the sodium salt of a 12-carbon organosulfate, with the chemical formula of $CH_3(CH_2)_{11}OSO_3Na$ (Figure 4a). The hydrocarbon tail with a polar headgroup results in amphiphilic properties, allowing SDS to act as a surfactant [50]. In the work by Jiang et al., 0.2 wt% CNTs was dispersed in water with 0.01 wt% SDS. The stability of the CNTs was evaluated using a UV–visible (UV–vis) scanning spectrophotometer that could measure the concentration of CNTs by fitting the absorbance to the calibration curve [49]. Figure 4b shows the concentration of CNTs with and without SDS as a function of the sedimentation time. The concentration of CNTs without SDS rapidly decreased as the sedimentation time increased. This decrease was not significant for CNTs with 0.1 wt% SDS. In general, a high concentration of CNTs indicates a better dispersion state of CNTs in a solvent. Therefore, the abovementioned observations indicated that the addition of SDS can help to enhance the dispersibility of CNTs in water. This improvement in the dispersibility was attributable to the high negative surface charge and steric hindrance resulting from the hydrophobic segment that promoted the interaction between CNTs and SDS. These results highlighted that surfactants such as SDS consisting of a hydrophobic segment with a single, long, straight-chain, and terminal hydrophilic head can effectively enhance the dispersibility of CNTs in water.

Li et al. used different types of surfactants such as SDS and octyl phenol ethoxylate (Triton X-100; TX100) to enhance the dispersibility of MWCNTs in water [51]. TX 100 ($C_{14}H_{22}O(C_2H_4O)_n(_{n=9–10})$) is a non-ionic surfactant consisting of a hydrophilic polyethylene oxide chain and an aromatic hydrocarbon lipophilic or hydrophobic group (Figure 5a). The CNT concentration was evaluated using a UV–vis spectrometer. Specifically, 20 mg of MWCNTs was dispersed in 40 mL of water with different contents of SDS and TX 100. Figure 5b shows the CNT concentrations for different contents of SDS and TX 100. The highest CNT concentration corresponded to the CNT suspension with 2000 mg/L TX 100. The excellent dispersibility of CNTs in water was attributable to the benzene ring structure in the tail group of TX100 [51]. In contrast, the sedimentation stability resulting from SDS was higher than that of TX 100. Figure 5c shows the sedimentation kinetics of MWCNTs dispersed in water with different surfactants (2000 mg/L) as a function of the sedimentation time. The y-axis shows the ratio of the measured height of the suspension to the initial height, with higher y values indicating lower sedimentation. The MWCNTs with SDS exhibited the slowest sedimentation. The addition of SDS increased the absolute values of the zeta potential (Figure 5d), resulting in enhanced stability [51]. Overall, different surfactants were associated with different benefits: non-ionic and anionic surfactants were more effective in enhancing the dispersibility and sedimentation stability, respectively.

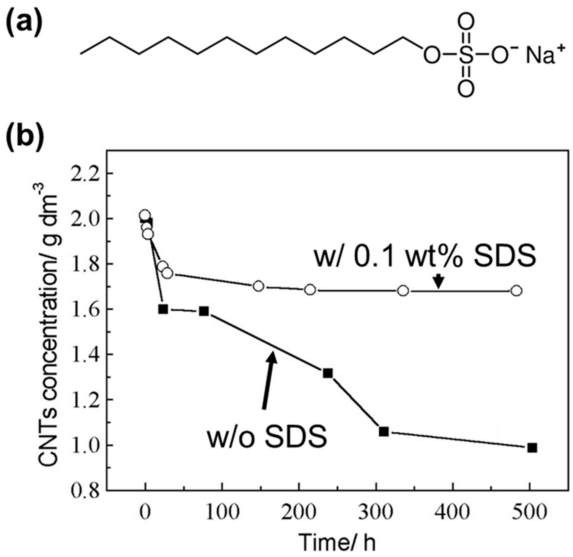


**Figure 4.** (**a**) Chemical structure of SDS and (**b**) CNT concentrations vs. time for 0.2 wt% CNT suspensions without SDS and with 0.1 wt% SDS at pH 9 [49]. Reproduced with permission [49] (Elsevier, 2003).

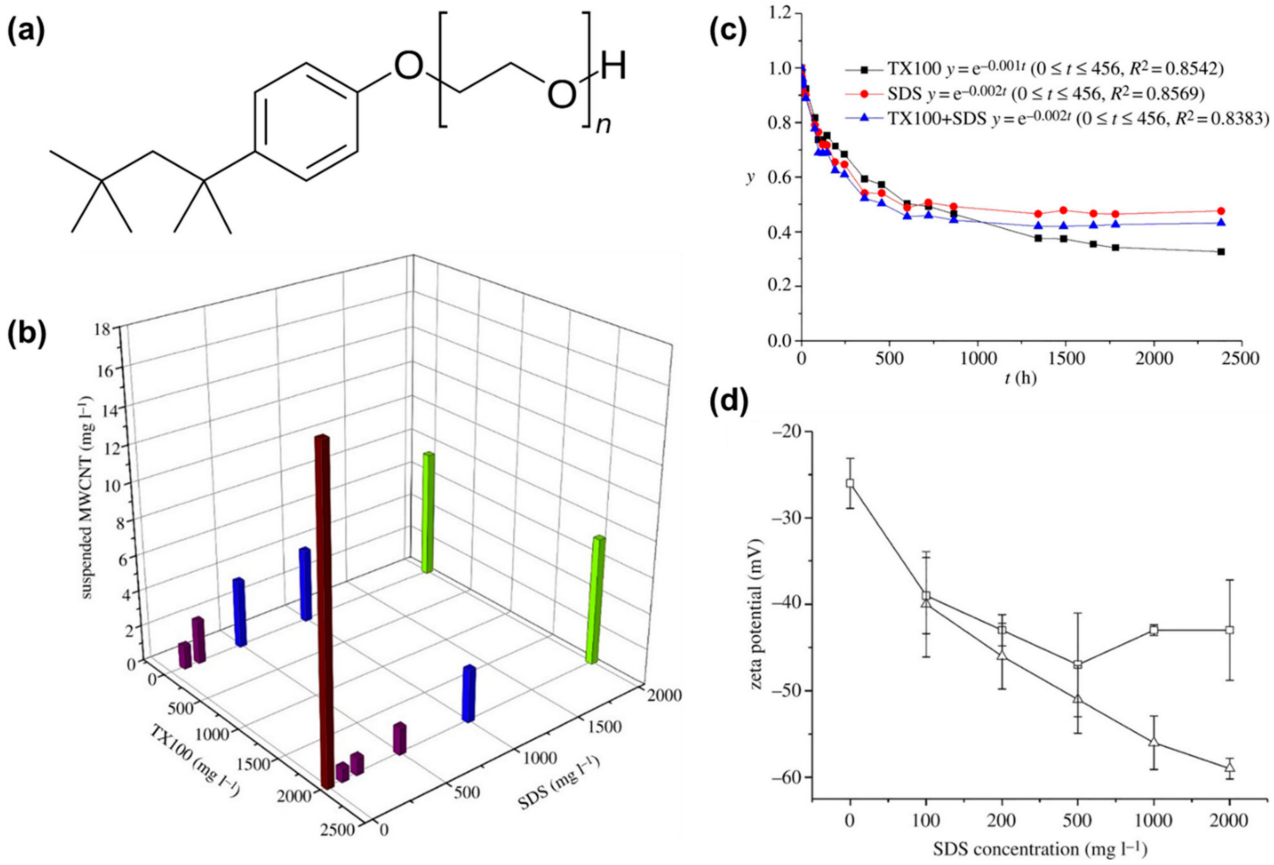


**Figure 5.** (**a**) Chemical structure of TX100. (**b**) Dispersibility of CNT concentrations with TX100 and SDS. (**c**) Sedimentation kinetics of MWCNT suspensions dispersed using single or mixed surfactants. The abscissa is the sedimentation time elapsed ($t$); $y$ indicates the ratio of the absorbance of the MWCNT suspension at time $t$ to that at the initial time. (**d**) Zeta potentials of MWCNT suspensions dispersed using single or mixed surfactants [51]. Reproduced with permission [51] (Royal Society Publishing, 2019).

Bai et al. compared the dispersibility of aqueous MWCNT suspensions with different types of surfactants, namely, SDS, TX 100, and hexadecyltrimethylammonium bromide (CTAB) [52]. CTAB ($(C_{16}H_{33})N(CH_3)_3$) (Figure 6a) is a cation surfactant consisting of bromide salt. In this study, 10 mg of MWCNTs was dispersed in 50 mL of water with 1 wt% surfactants. The dispersibility of the MWCNT suspension with the different surfactants was evaluated using a UV–vis spectrometer. Figure 6b shows the dispersibility of MWCNTs with the different surfactants. The highest and lowest dispersibility of MWCNTs was achieved using TX 100 and CTAB, respectively. The performance of SDS and dioctylsulfosuccinate sodium (AOT) was similar to that with CTAB. In general, the benzene rings of TX 100 enhance the absorption properties of MWCNTs [53,54]; thus, TX 100 having a benzene unit magnified the attraction to the MWCNTs, thereby enhancing the dispersibility of MWCNTs in water. Because SDS and CTAB do not have aromatic units, the adsorption capability to the surface of MWCNTs was weaker than that of TX 100. The dispersibility is also influenced by the chain length of the tail. Longer chain lengths result in larger spatial volume, thereby generating more repulsive forces between the individual MWCNTs owing to the higher steric hindrance. The tail chain length of SDS is higher than that of CTAB; therefore, the MWCNT suspension with SDS exhibited slightly higher dispersibility than that with CTAB. Overall, surfactants having benzene rings helped to enhance the dispersibility. Among the surfactants without benzene rings, surfactants with long chain length of the tail were more effective in enhancing the dispersibility of MWCNTs in water.

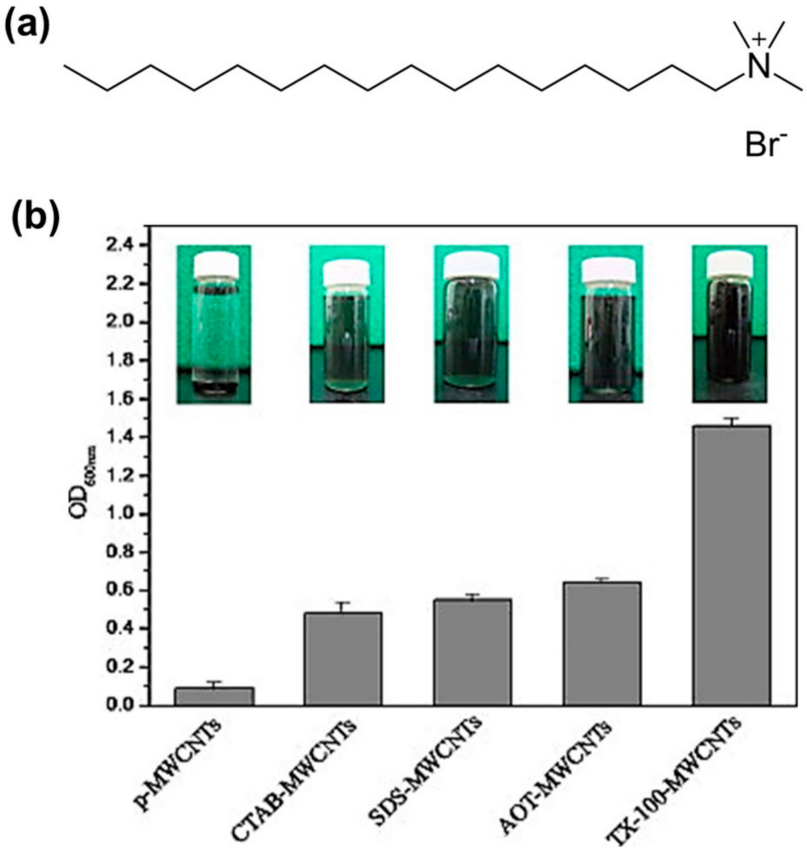


**Figure 6.** (**a**) Chemical structure of CTAB and (**b**) the dispersion ability of p-MWCNTs and different surfactant-modified MWCNTs detected using a UV–vis spectrophotometer at 600 nm [52]. Reproduced with permission [52] (Elsevier, 2011).

In the work by Islam et al., 0.1 mg/mL SWCNTs was dispersed in water with another anionic surfactant, sodium dodecylbenzenesulfonate (SDBS) [55]. SDBS ($C_{18}H_{29}NaO_3S$) has a long chain length of the tail and aromatic units (Figure 7a); thus, it was expected to

enhance the dispersibility of SWCNTs in water. The dispersibility of SWCNTs in water with different surfactants, namely, TX 100, SDS, and SDBS, was evaluated. Figure 7b shows the image of the SWCNT suspensions with the different surfactants after two months. The highest and lowest dispersion stability of the SWCNT suspension corresponded to the samples with SDBS and SDS, respectively. The aromatic rings in SDBS promoted absorption to the surface of the SWCNTs, which helped to enhance the dispersion stability. In addition, SDBS has a long chain length of the tail, which helped to enhance the dispersion stability by increasing the steric hindrance.

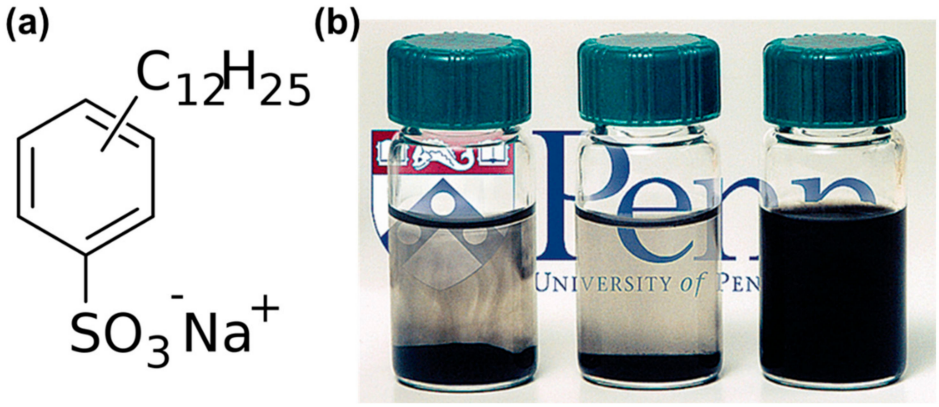


**Figure 7.** (**a**) Chemical structure of SDBS and (**b**) vials (6 mL) containing aqueous CNT dispersions with (left to right) SDS, TX100, and SDBS. SDS and TX100 samples were imaged after sitting for 5 days, whereas SDBS samples were imaged after 2 months of sitting at room temperature. SDBS-CNT suspensions appeared homogeneous, whereas SDS and TX100-CNT suspensions had coagulated nanotubes in the body and at the bottom of the vials [55]. Reproduced with the permission of Ref. [55] (American Chemical Society, 2018).

In the work by Rastogi et al., the dispersibility of MWCNTs was compared using the other non-ionic surfactants, Tween 20 ($C_{58}H_{114}O_{26}$) and Tween 80 ($C_{64}H_{124}O_{26}$) [56]. Tween 20 (Figure 8a) and Tween 80 (Figure 8b) have longer hydrocarbon tails than SDS and Tx100. In total, 50 mg/L MWCNTs was mixed in water with four different surfactants at 1 wt%, including SDS, Tween 20, Tween 80, and TX 100. The dispersibility was evaluated using a UV-vis spectrometer. Figure 8c–f show the UV–vis spectra of MWNT suspensions with different surfactants at varying concentrations. MWCNTs with TX 100 showed the highest absorbance among those with other surfactants, while the minimum absorbance was observed in MWCNTs with SDS. Tween 80 and Tween 20 showed similar absorbance. Therefore, the order of dispersibility was confirmed to be SDS < Tween 20/Tween 80 < TX 100. In aqueous CNT dispersions, the hydrophobic tails of surfactants attach to the surface of CNTs, while the hydrophilic heads interact with the aqueous phase, thereby lowering the interfacial tension between CNT surface and water. Therefore, the dispersibility of an MWCNT suspension is highly governed by the degree of adsorption of surfactants on the surface of CNTs as well as that of steric hindrance by the chain length of the tail. The molecules with the aromatic units are more effectively adsorbed on the surface of graphite through $\pi$–$\pi$ interactions [56]. Meanwhile, Tween 80 and Tween 20 have longer chain length of hydrocarbon tail than SDS and TX 100. Considering the steric hindrance, TX 100 was expected to show the worst dispersibility because the effective chain length of TX 100 is the shortest among the used surfactants, which was not consistent with the experimental results. This was attributed to the existence of aromatic units in TX 100. Therefore, it confirmed that the "benzene ring factor" is more effective than the "tail length factor" in enhancing the dispersibility of CNTs in water.

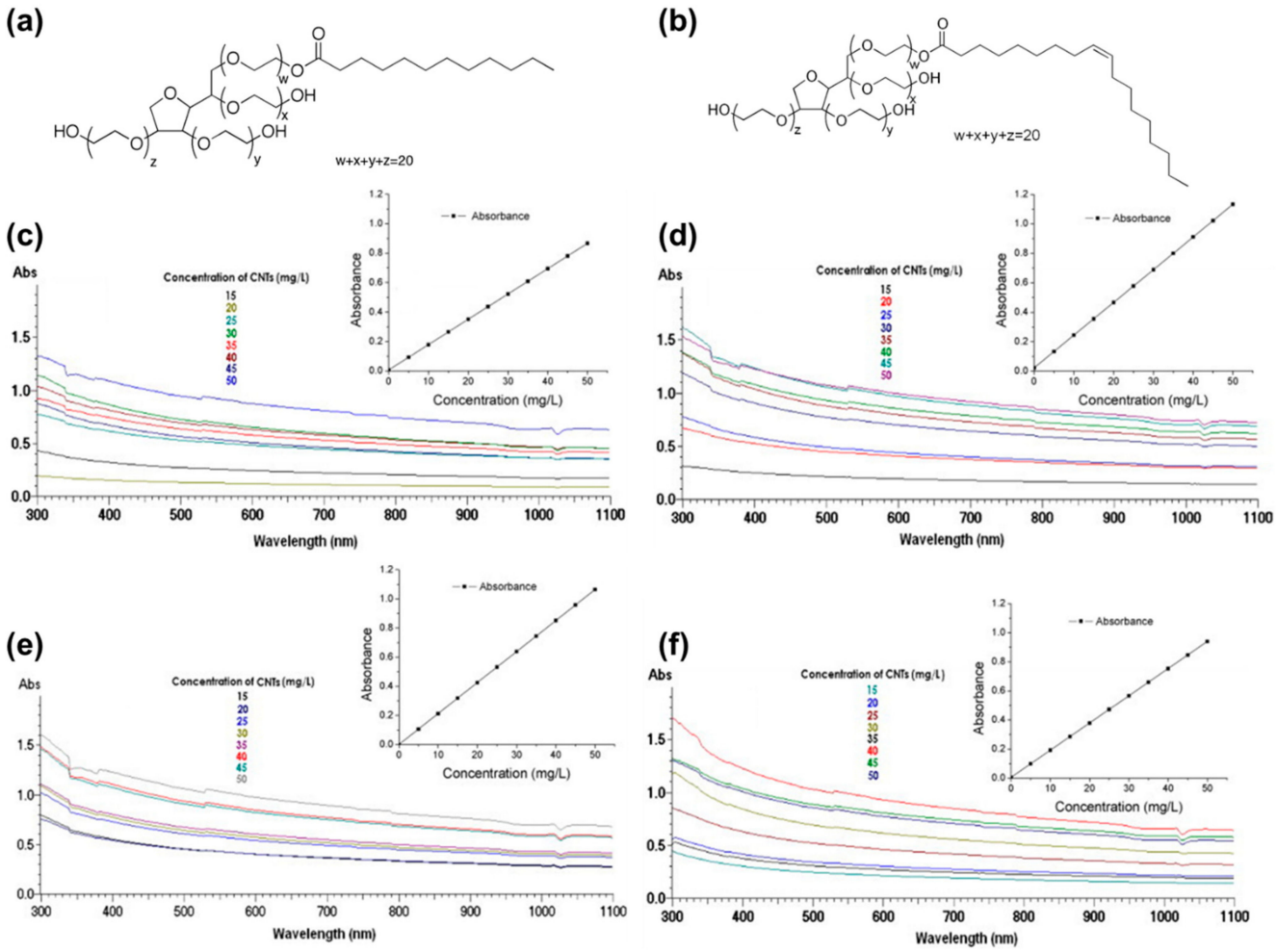


**Figure 8.** Chemical structures of (**a**) Tween 20 and (**b**) Tween 80. UV–vis spectra of MWCNT suspensions with (**c**) SDS, (**d**) Tween 80, (**e**) Tween 20, and (**f**) Triton X-100 [56]. Reproduced with permission [56] (Elsevier, 2008).

To expand the versatility of CNTs, there have been various efforts to enhance the dispersibility of CNTs in organic solvents such as ethanol, N-Methyl-2-pyrrolidone (NMP), etc. In the work by Bricha et al. [57], five types of surfactants (CTAB as a cationic surfactant, SDS as an anionic surfactant, and TX100, Pluronic F-127, and Span 60 ($C_{24}H_{46}O_6$) as non-ionic surfactants) were selected to enhance the dispersibility of MWCNTs in ethanol (Figure 9a). In this work, the concentration of the MWCNT dispersion was constant, at 1 g/L, and the MWCNT dispersions with 10 wt% surfactants were sonicated for 3 h. To evaluate the performance of surfactants, they characterized the zeta potential value according to the time, as shown in Figure 9b. Although Span 60 has a longer length of tail groups than SDS, the absolute zeta potential value of the MWCNTs with SDS showed to be higher. It indicated that SDS could prevent the agglomerations of MWCNTs, and the double bonds in the tail group were more effective in enhancing the dispersibility of MWCNTs in ethanol than the length of the tail group. Furthermore, the absolute zeta potential value of TX 100 was higher than that of CTAB after 24 h, and the value of CTAB was decreased dramatically. Through comparing the results of CTAB and TX100, the phenyl structures were more helpful in improving the dispersion stability of MWCNTs than the tail length.

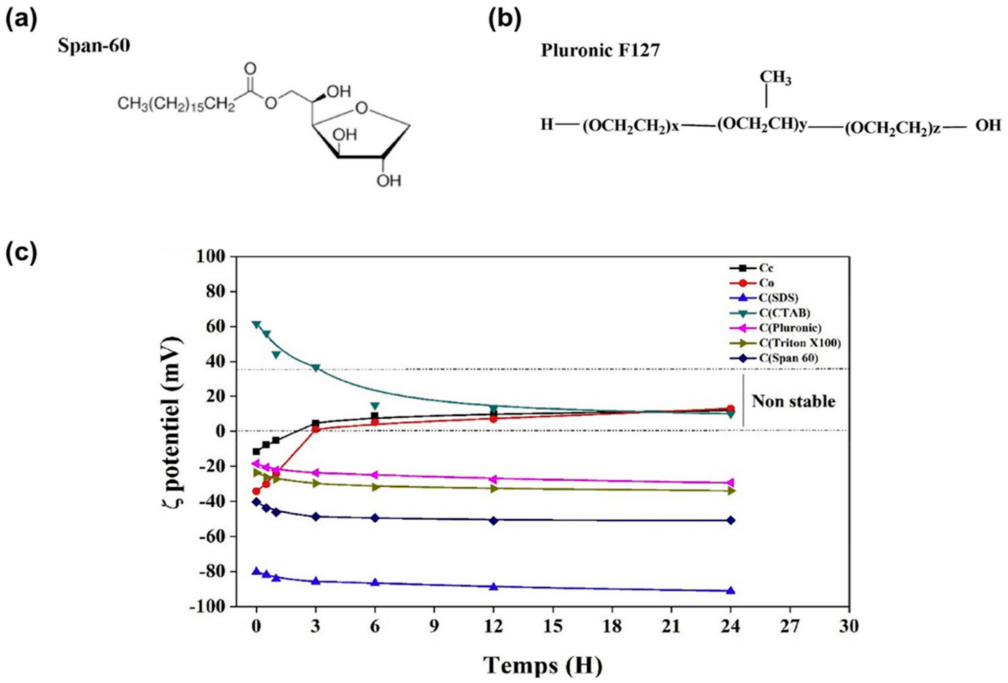


**Figure 9.** Chemical structures of (**a**) Span-60 and (**b**) Pluronic F127. (**c**) Zeta potential results of CNT dispersions with various types of surfactants according to the time [57]. Reproduced with permission [57] (Elsevier, 2019).

NMP is widely used as an organic solvent to fabricate the slurry for the electrodes of batteries. In the work by Goh et al. [58], the dispersibility of MWCNTs in NMP was characterized depending on the charged types of surfactants, including SDS, CTAB, and TX 100. They mixed 0.5 g of MWCNTs and 100 mL of the aqueous solution with 1 wt% of various surfactants to make surfactant-treated MWCNTs. After sonication for 1 h, the treated MWCNTs were filtered and dried at 60 °C. An amount of 0.05 g of fabricated MWCNTs was dispersed in 15 mL of NMP; then, they compared the stability of the MWCNT dispersions according to the surfactants. As a result, the pristine MWCNT dispersion and the CTAB-treated MWCNT dispersion showed poor stability in SMP. In the case of MWCNTs with SDS, although the sedimentation of MWCNTs was much lower than that in the pristine and CTAB cases, there was a slight sedimentation of MWCNTs. However, the MWCNTs with TX 100 showed the best dispersion stability compared with other surfactants, because the hydrophilic polyethylene glycol groups of TX 100 have a polarity similar to that of NMP, which showed a more effective interaction between TX 100 and NMP than other surfactants. Therefore, TX 100 is a promising candidate when MWCNTs are dispersed in NMP.

The polymer wrapping on the surface of CNTs can also assist in dispersing CNTs in organic solvents. Several types of polymers, such as conjugated polymers, can be made to interact with the surface of CNTs via van der Waals forces [59]. The efficiency of polymer dispersants can be dependent on the chain length and the structure of chains of the conjugated polymer. Gomulya et al. [60] utilized a polyfluorene-based polymer with different alkyl chain lengths, from $C_6H_{13}$ (PF6) to $C_{18}H_{37}$ (PF18), for dispersing SWCNTs in toluene. Figure 10a shows the absorption spectra of polymer-wrapped SWCNT dispersions with different alkyl chain lengths. Regardless of the size of the CNTs, the optical density was increased with the increase in the alkyl chain length, which indicated that the polymer with a longer chain length could be wrapped more efficiently and restrict the aggregation of CNTs. Furthermore, for investigating the effect of the chain length of polymers, they conducted a molecular dynamic simulation, which is the simulation method for analyzing the movement of the molecules and predicting the phenomenon based on Newton's equations of motion. As shown in Figure 10b, there were SWCNTs with three

different types of polymers, namely, PF12, PF15, and PF18, from top to bottom, respectively. The left side and right side of the figures show the vertical and parallel directions of the polymer backbones to the surface of the CNTs. In the case of the SWCNTs with PF12, there were the enough sites to be attached to other chains. PF15 was attached well to CNTs in both directions, which indicated that a longer chain length of the polymer was more favorable to cover the surface of SWCNTs. However, in the case of PF18, although the polymer chains were covered well in the vertical direction, the chains were detached from the surface of the SWCNTs in the parallel direction. Through the simulation, we can predict how molecules will behave.

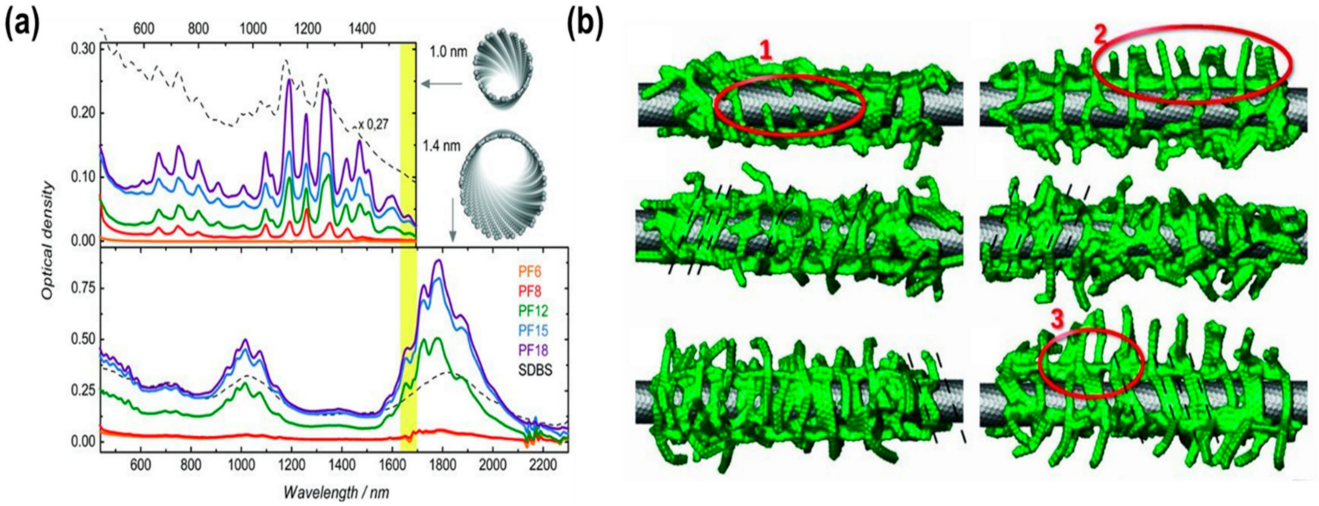


**Figure 10.** (**a**) Absorption spectra of the SWCNT dispersions in toluene according to the alkyl chain length of the polyfluorene derivatives and (**b**) molecular dynamic simulations of SWCNTs with PF12, PF15, and PF18, from top to bottom, respectively. The left side and right side of figures show the vertical and parallel directions of the polymer backbones to the surface of the CNTs [60]. Reproduced with permission [60] (John Wiley and Sons, 2013).

Finally, we report the research studies that described the relationship between the presence of surfactants and the electrochemical performance of batteries to emphasize the importance of surfactants in CNT dispersion and battery applications. Lassi et al. demonstrated that the presence of a surfactant in a CNT suspension enhanced the performance of a lithium-ion battery [61]. They increased the conductivity of lithium iron phosphate ($LiFePO_4$, LFP) via introducing polyoxyethylene-oleyl ether (E-230) with the chemical formula of $C_{18}H_{35}O$-$(C_2H_4O)_n$-H as a non-ionic surfactant. At first, they mixed an LFP solution and MWCNT dispersion with or without E-230 in water and then dried the mixture to obtain the LFP-MWCNT powder as an active material. They fixed 0.315 g of LFP and 0.018 g of MWCNTs and changed the amount of the surfactant from 0 g (E0) to 0.253 g (E5). After the fabrication of the active material, they dispersed the active material, Super P, and binder in NMP in a mass ratio of 16:3:1, respectively. They measured the electrochemical performance of the battery through coin cells with the fabricated LFP-MWCNT electrode, lithium metal foil as the counter electrode, and 1 M LiPF6 as the electrolyte. The specific capacity at a 0.2C rate of E5 (115 mAh/g) showed to be higher than that of E0 (89 mAh/g). This indicated that applying a surfactant to disperse MWCNTs uniformly assisted in enhancing the specific capacitance and cycle stability of the battery and showed the importance of surfactants. In the work by Wang et al. [62], a composite with silicone and CNTs (Si@C-CNTs) was fabricated for the anode of a lithium-ion battery. They demonstrated that the presence of SDS as a surfactant had the advantage of improving the performance of the battery using the Si@C-CNTs composite. They prepared a Si/CNT dispersion by introducing 1 g of SDS in 15 g of CNT dispersion with 0.4 wt% CNTs and then centrifuging the dispersion to obtain SDS-treated CNTs. After that, they redispersed the SDS-treated

CNTs in ethanol and mixed the CNT dispersion with a silicone dispersion. Then, after a gelatin solution was added into the Si/CNTs solution, the mixture of gelatin with Si/CNTs solution was pyrolyzed at 500 °C for 6 h in an Ar atmosphere. The obtained Si@C-CNT composites were named according to the mass ratio of silicone nanoparticle, the gelatin, and CNTs, and WS described the composite without the use of the SDS surfactant. For the measure the electrochemical performance of the coin cell battery, they mixed Si@C-CNTs, acetylene black as conductive agents, and polyvinylidene fluoride (PVDF) as the binder in a mass ratio of 7:2:1, respectively. The used electrolyte was 1 M LiPF6 in the solution with ethylene carbonate (1): diethyl carbonate (1): ethylene methyl carbonate (1); they utilized lithium foil as the counter electrode. As shown in Figure 11a, the discharge capacity of both the composites named Si@C-CNTs-5-0-0 and Si@C-CNTs-5-4-1-WS showed a sharp decline, even before 20 cycles, because both composites had low electrical conductivity and were unstable. However, using SDS in the Si@C-CNTs-5-4-1 composite showed a more stable cycle performance than the composite without SDS (Figure 11b). Furthermore, the initial capacity of the composite with SDS was much higher than that of the composite without SDS. These results imply that the presence of SDS and a homogeneous CNT dispersion can enhance the capacity and cycle stability of a battery and that the use of surfactants accounts for a significant portion.

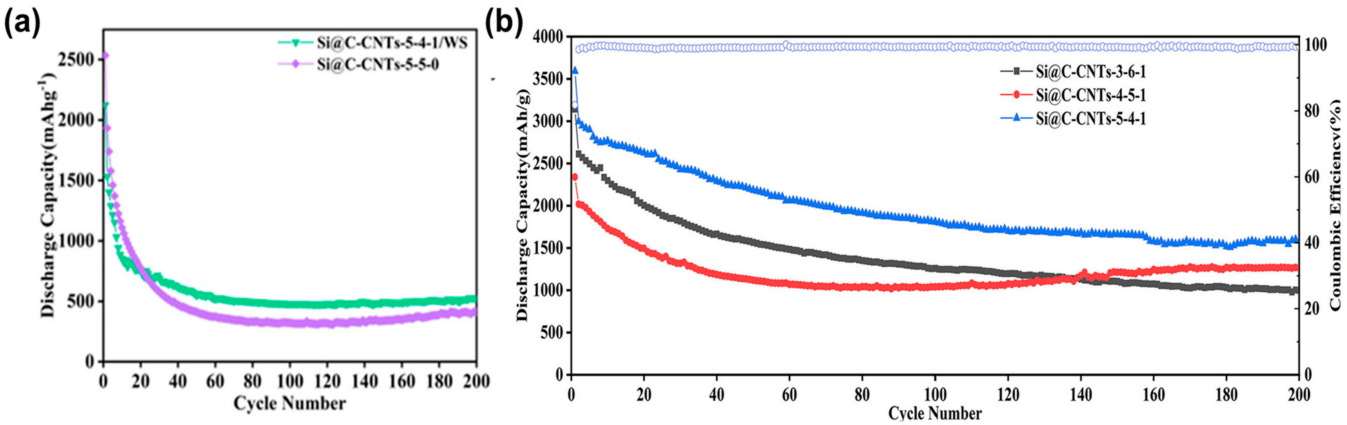


**Figure 11.** (**a**) Cycle performance of the battery with (**a**) Si@C-CNTs-5-4-1/WS and Si@C-CNTs-5-5-0, and (**b**) Si@C-CNTs-3-6-1, Si@C-CNTs-4-5-1, and Si@C-CNTs-5-4-1 [62]. Reproduced with permission [62] (Elsevier, 2022).

## 3. Summary

This paper summarizes and discusses the dispersibility of CNTs with different surfactants. Table 1 presents the comparison of CNT suspension using different surfactants. Surfactants with aromatic units show good absorption capability on the surface of CNTs, which enhances the dispersibility of the CNT suspension. The long chain length of the tail of a surfactant is effective in enhancing the dispersibility by promoting repulsion through the increase in the steric hindrance. Consequently, TX 100 and SDBS, which have aromatic units, lead to a higher dispersibility than that achieved using SDS or CTAB, which has no aromatic units. The dispersibility of SDS is higher than that of CTAB owing to their longer chain length of the tail.

Although the dispersibility of CNTs using various surfactants has been widely studied, systematic studies on the sedimentation of CNTs using different types of surfactants are lacking. The sedimentation of CNTs is governed by complex mechanisms. Therefore, future studies must focus on the sedimentation behavior of CNTs with different surfactants to comprehensively understand the stability of CNTs.

**Table 1.** Surfactants to enhance CNT dispersibility.

| Material | Type | Aromatic Unit | Solvent | Dispersibility | Ref. |
|---|---|---|---|---|---|
| SDS | Anionic | No | Water | Moderate | [49,51,52] |
| | | | Ethanol | Excellent | [57] |
| | | | NMP | Good | [58] |
| CTAB | Cationic | No | Water | Moderate | [52] |
| | | | Ethanol | Bad | [57] |
| | | | NMP | Bad | [58] |
| AOT | Anionic | No | Water | Moderate | [52] |
| Tween 20 | Non-ionic | No | Water | Good | [56] |
| Tween 80 | Non-ionic | No | Water | Good | [56] |
| TX 100 | Non-ionic | Yes | Water | Excellent | [51,52,63] |
| | | | Ethanol | Good | [57] |
| | | | NMP | Excellent | [58] |
| SDBS | Anionic | Yes | Water | Excellent | [63] |
| Span 60 | Non-ionic | No | Ethanol | Excellent | [57] |
| Pluronic F127 | Non-ionic | No | Ethanol | Good | [57] |
| PF6 | Polymer | Yes | Toluene | Bad | [60] |
| PF8 | | | | Moderate | |
| PF12 | | | | Good | |
| PF15 | | | | Excellent | |
| PF18 | | | | Excellent | |

Furthermore, we show that the use of surfactants can improve the performance of the battery by enhancing the dispersibility of CNTs in solvents. Although it has been demonstrated that well-dispersed CNTs in solvents improve the battery performance, there are few studies on the performance evaluation of batteries according to the presence and types of surfactants. Because there are various surfactants, research on appropriate surfactants depending on the solvents is also considered important. Moreover, as research on various substrates with flexibility and active materials has been conducted actively on next-generation batteries, there is a possibility that the importance of surfactants and the method to increase the dispersibility of CNTs will increase in the future.

**Author Contributions:** Conceptualization, H.Y., H.K. and B.H.; methodology, H.Y., H.K. and B.H.; formal analysis, H.Y. and H.K.; investigation, H.Y. and H.K.; resources, B.H.; data curation, H.Y., H.K. and B.H.; writing—original draft preparation, H.Y., H.K., P.M. and B.H.; writing—review and editing, H.Y., H.K, P.M. and B.H.; visualization, H.Y. and B.H.; supervision, B.H.; project administration, B.H.; funding acquisition, B.H. All authors have read and agreed to the published version of the manuscript.

**Funding:** This work was supported by National Research Foundation of Republic of Korea (NRF-2022R1F1A1063696). This research was supported by Chung-Ang University Graduate Research Scholarship in 2022.

**Informed Consent Statement:** Not applicable.

**Data Availability Statement:** Not applicable.

**Acknowledgments:** This work was supported by National Research Foundation of Republic of Korea (NRF-2022R1F1A1063696). This research was supported by Chung-Ang University Graduate Research Scholarship in 2022.

**Conflicts of Interest:** The authors declare no conflict of interest.

## References

1. Cheong, J.Y.; Lee, S.; Lee, J.; Lim, H.; Cho, S.-H.; Lee, D.C.; Kim, I.-D. $CuFeO_2$–$NiFe_2O_4$ hybrid electrode for lithium-ion batteries with ultra-stable electrochemical performance. *RSC Adv.* **2019**, *9*, 27257–27263. [CrossRef] [PubMed]
2. Hwang, B.; Han, Y.; Matteini, P. Bending fatigue behavior of Ag nanowire/Cu thin-film hybrid interconnects for wearable electronics. *Facta Univ. Ser. Mech. Eng.* **2022**. [CrossRef]
3. Ventrapragada, L.K.; Zhu, J.; Creager, S.E.; Rao, A.M.; Podila, R. A Versatile Carbon Nanotube-Based Scalable Approach for Improving Interfaces in Li-Ion Battery Electrodes. *ACS Omega* **2018**, *3*, 4502–4508. [CrossRef] [PubMed]

4. Wu, Z.; Liu, K.; Lv, C.; Zhong, S.; Wang, Q.; Liu, T.; Liu, X.; Yin, Y.; Hu, Y.; Wei, D. Ultrahigh-energy density lithium-ion cable battery based on the carbon-nanotube woven macrofilms. *Small* **2018**, *14*, 1800414. [CrossRef]
5. Lee, J.H.; Yoon, C.S.; Hwang, J.-Y.; Kim, S.-J.; Maglia, F.; Lamp, P.; Myung, S.-T.; Sun, Y.-K. High-energy-density lithium-ion battery using a carbon-nanotube–Si composite anode and a compositionally graded Li $[Ni_{0.85}\ Co_{0.05}\ Mn_{0.10}]\ O_2$ cathode. *Energy Environ. Sci.* **2016**, *9*, 2152–2158. [CrossRef]
6. Zhu, L.; Zhu, W.; Cheng, X.-B.; Huang, J.-Q.; Peng, H.-J.; Yang, S.-H.; Zhang, Q. Cathode materials based on carbon nanotubes for high-energy-density lithium–sulfur batteries. *Carbon* **2014**, *75*, 161–168. [CrossRef]
7. Hu, J.W.; Wu, Z.P.; Zhong, S.W.; Zhang, W.B.; Suresh, S.; Mehta, A.; Koratkar, N. Folding insensitive, high energy density lithium-ion battery featuring carbon nanotube current collectors. *Carbon* **2015**, *87*, 292–298. [CrossRef]
8. Landi, B.J.; Cress, C.D.; Raffaelle, R.P. High energy density lithium-ion batteries with carbon nanotube anodes. *J. Mater. Res.* **2010**, *25*, 1636–1644. [CrossRef]
9. Liu, X.-M.; dong Huang, Z.; woon Oh, S.; Zhang, B.; Ma, P.-C.; Yuen, M.M.; Kim, J.-K. Carbon nanotube (CNT)-based composites as electrode material for rechargeable Li-ion batteries: A review. *Compos. Sci. Technol.* **2012**, *72*, 121–144. [CrossRef]
10. Yuan, W.; Zhang, Y.; Cheng, L.; Wu, H.; Zheng, L.; Zhao, D. The applications of carbon nanotubes and graphene in advanced rechargeable lithium batteries. *J. Mater. Chem. A* **2016**, *4*, 8932–8951. [CrossRef]
11. Sun, S.; Yan, Q.; Wu, M.; Zhao, X. Carbon aerogel based materials for secondary batteries. *Sustain. Mater. Technol.* **2021**, *30*, e00342. [CrossRef]
12. Reddy, A.L.M.; Shaijumon, M.M.; Gowda, S.R.; Ajayan, P.M. Coaxial MnO2/carbon nanotube array electrodes for high-performance lithium batteries. *Nano Lett.* **2009**, *9*, 1002–1006. [CrossRef]
13. Guo, B.; Wang, X.; Fulvio, P.F.; Chi, M.; Mahurin, S.M.; Sun, X.G.; Dai, S. Soft-templated mesoporous carbon-carbon nanotube composites for high performance lithium-ion batteries. *Adv. Mater.* **2011**, *23*, 4661–4666. [CrossRef]
14. Nossol, E.; Souza, V.H.; Zarbin, A.J. Carbon nanotube/Prussian blue thin films as cathodes for flexible, transparent and ITO-free potassium secondary battery. *J. Colloid Interface Sci.* **2016**, *478*, 107–116. [CrossRef]
15. Liu, L.; Cheng, M.; Yang, Z. Improved performance of flower-like ZnAl LDH growing on carbon nanotubes used in zinc–nickel secondary battery. *Electrochim. Acta* **2018**, *277*, 67–76. [CrossRef]
16. Kim, T.; Mo, Y.; Nahm, K.; Oh, S.M. Carbon nanotubes (CNTs) as a buffer layer in silicon/CNTs composite electrodes for lithium secondary batteries. *J. Power Sources* **2006**, *162*, 1275–1281. [CrossRef]
17. Lee, S.W.; Yabuuchi, N.; Gallant, B.M.; Chen, S.; Kim, B.-S.; Hammond, P.T.; Shao-Horn, Y. High-power lithium batteries from functionalized carbon-nanotube electrodes. *Nat. Nanotechnol.* **2010**, *5*, 531–537. [CrossRef]
18. Luo, Y.; Wang, K.; Li, Q.; Fan, S.; Wang, J. Macroscopic carbon nanotube structures for lithium batteries. *Small* **2020**, *16*, 1902719. [CrossRef]
19. Qaiser, N.; Al-Modaf, F.; Khan, S.M.; Shaikh, S.F.; El-Atab, N.; Hussain, M.M. A Robust Wearable Point-of-Care CNT-Based Strain Sensor for Wirelessly Monitoring Throat-Related Illnesses. *Adv. Funct. Mater.* **2021**, *31*, 2103375. [CrossRef]
20. Mun, J.; Park, J.-H.; Choi, W.; Benayad, A.; Park, J.-H.; Lee, J.-M.; Doo, S.-G.; Oh, S.M. New dry carbon nanotube coating of over-lithiated layered oxide cathode for lithium ion batteries. *J. Mater. Chem. A* **2014**, *2*, 19670–19677. [CrossRef]
21. Wang, K.; Wu, Y.; Luo, S.; He, X.; Wang, J.; Jiang, K.; Fan, S. Hybrid super-aligned carbon nanotube/carbon black conductive networks: A strategy to improve both electrical conductivity and capacity for lithium ion batteries. *J. Power Sources* **2013**, *233*, 209–215. [CrossRef]
22. Hai, N.Q.; Kim, H.; Yoo, I.S.; Hur, J. Facile and scalable preparation of a $MoS_2$/carbon nanotube nanocomposite anode for high-performance lithium-ion batteries: Effects of carbon nanotube content. *J. Nanosci. Nanotechnol.* **2019**, *19*, 1494–1499. [CrossRef] [PubMed]
23. Choi, Y.; Cho, S.; Lee, Y.-S. Effect of the addition of carbon black and carbon nanotube to $FeS_2$ cathode on the electrochemical performance of thermal battery. *J. Ind. Eng. Chem.* **2014**, *20*, 3584–3589. [CrossRef]
24. Qaiser, N.; Kim, Y.J.; Hong, C.S.; Han, S.M. Numerical Modeling of Fracture-Resistant Sn Micropillars as Anode for Lithium Ion Batteries. *J. Phys. Chem. C* **2016**, *120*, 6953–6962. [CrossRef]
25. Palanisamy, R.; Karuppiah, D.; Venkatesan, S.; Mani, S.; Kuppusamy, M.; Marimuthu, S.; Karuppanan, A.; Govindaraju, R.; Marimuthu, S.; Rengapillai, S.; et al. High-performance asymmetric supercapacitor fabricated with a novel MoS2/Fe2O3/Graphene composite electrode. *Colloid Interface Sci. Commun.* **2022**, *46*, 100573. [CrossRef]
26. Kapiamba, K.F. Mini-review of the microscale phenomena during emulsification of highly concentrated emulsions. *Colloid Interface Sci. Commun.* **2022**, *47*, 100597. [CrossRef]
27. Islam, M.S.; Mitra, S. Development of nano structured graphene oxide incorporated dexamethasone with enhanced dissolution. *Colloid Interface Sci. Commun.* **2022**, *47*, 100599. [CrossRef]
28. Singh, M.; Rana, S.; Singh, A.K. Advanced nanomaterials utilized as top transparent electrodes in semi-transparent photovoltaic. *Colloid Interface Sci. Commun.* **2022**, *46*, 100563. [CrossRef]
29. Abbasi Moud, A. Recent advances in utility of artificial intelligence towards multiscale colloidal based materials design. *Colloid Interface Sci. Commun.* **2022**, *47*, 100595. [CrossRef]
30. Kim, T.; Kim, J.; Hyun, S.; Han, S.M. Fabrication of ultralight 3D porous composite for Ag nanowire/cellulose nanofiber with tunable mechanical and electrical properties via directional freeze casting. *Extrem. Mech. Lett.* **2019**, *30*, 100512. [CrossRef]

31. Hu, C.Y.; Xu, Y.J.; Duo, S.W.; Zhang, R.F.; Li, M.S. Non-covalent functionalization of carbon nanotubes with surfactants and polymers. *J. Chin. Chem. Soc.* **2009**, *56*, 234–239. [CrossRef]
32. Hofstra, A.A.; Morris, M.L.; Sample, J.L.; Powell, W.D. Non-covalent functionalized nanotubes in nylon 12. *Phys. Chem. Interfaces Nanomater. VI SPIE* **2007**, 7–15. [CrossRef]
33. Saleemi, M.A.; Fouladi, M.H.; Yong, P.V.C.; Wong, E.H. Elucidation of antimicrobial activity of non-covalently dispersed carbon nanotubes. *Materials* **2020**, *13*, 1676. [CrossRef]
34. Tuncel, D. Non-covalent interactions between carbon nanotubes and conjugated polymers. *Nanoscale* **2011**, *3*, 3545–3554. [CrossRef]
35. Chen, G.-X.; Li, Y.; Shimizu, H. Ultrahigh-shear processing for the preparation of polymer/carbon nanotube composites. *Carbon* **2007**, *45*, 2334–2340. [CrossRef]
36. Andrews, R.; Jacques, D.; Minot, M.; Rantell, T. Fabrication of carbon multiwall nanotube/polymer composites by shear mixing. *Macromol. Mater. Eng.* **2002**, *287*, 395–403. [CrossRef]
37. Thostenson, E.T.; Chou, T.-W. Aligned multi-walled carbon nanotube-reinforced composites: Processing and mechanical characterization. *J. Phys. D Appl. Phys.* **2002**, *35*, L77. [CrossRef]
38. Luo, Z.; Koo, J. Quantitative study of the dispersion degree in carbon nanofiber/polymer and carbon nanotube/polymer nanocomposites. *Mater. Lett.* **2008**, *62*, 3493–3496. [CrossRef]
39. Gupta, M.L.; Sydlik, S.A.; Schnorr, J.M.; Woo, D.J.; Osswald, S.; Swager, T.M.; Raghavan, D. The effect of mixing methods on the dispersion of carbon nanotubes during the solvent-free processing of multiwalled carbon nanotube/epoxy composites. *J. Polym. Sci. Part B: Polym. Phys.* **2013**, *51*, 410–420. [CrossRef]
40. Hwang, B.; An, Y.; Lee, H.; Lee, E.; Becker, S.; Kim, Y.-H.; Kim, H. Highly Flexible and Transparent Ag Nanowire Electrode Encapsulated with Ultra-Thin Al2O3: Thermal, Ambient, and Mechanical Stabilities. *Sci. Rep.* **2017**, *7*, 41336. [CrossRef]
41. Inam, F.; Vo, T.; Jones, J.P.; Lee, X. Effect of carbon nanotube lengths on the mechanical properties of epoxy resin: An experimental study. *J. Compos. Mater.* **2013**, *47*, 2321–2330. [CrossRef]
42. Cheng, Q.; Debnath, S.; Gregan, E.; Byrne, H.J. Ultrasound-assisted SWNTs dispersion: Effects of sonication parameters and solvent properties. *J. Phys. Chem. C* **2010**, *114*, 8821–8827. [CrossRef]
43. Montazeri, A.; Chitsazzadeh, M. Effect of sonication parameters on the mechanical properties of multi-walled carbon nanotube/epoxy composites. *Mater. Des. (1980–2015)* **2014**, *56*, 500–508. [CrossRef]
44. Yang, K.; Yi, Z.; Jing, Q.; Yue, R.; Jiang, W.; Lin, D. Sonication-assisted dispersion of carbon nanotubes in aqueous solutions of the anionic surfactant SDBS: The role of sonication energy. *Chin. Sci. Bull.* **2013**, *58*, 2082–2090. [CrossRef]
45. Montazeri, A.; Montazeri, N.; Pourshamsian, K.; Tcharkhtchi, A. The effect of sonication time and dispersing medium on the mechanical properties of multiwalled carbon nanotube (MWCNT)/epoxy composite. *Int. J. Polym. Anal. Charact.* **2011**, *16*, 465–476. [CrossRef]
46. Gao, S.; Villacorta, B.S.; Ge, L.; Rufford, T.E.; Zhu, Z. Effect of sonication and hydrogen peroxide oxidation of carbon nanotube modifiers on the microstructure of pitch-derived activated carbon foam discs. *Carbon* **2017**, *124*, 142–151. [CrossRef]
47. Meng, Y.; Liao, B.; Pang, H.; Zhang, J.; Song, L. Cyclodextrin-modified polycarboxylate superplasticizers as dispersant agents for multiwalled carbon nanotubes. *J. Appl. Polym. Sci.* **2019**, *136*, 47311. [CrossRef]
48. Soleimani Zohr Shiri, M.; Henderson, W.; Mucalo, M.R. A Review of The Lesser-Studied Microemulsion-Based Synthesis Methodologies Used for Preparing Nanoparticle Systems of The Noble Metals, Os, Re, Ir and Rh. *Materials* **2019**, *12*, 1896. [CrossRef]
49. Jiang, L.; Gao, L.; Sun, J. Production of aqueous colloidal dispersions of carbon nanotubes. *J. Colloid Interface Sci.* **2003**, *260*, 89–94. [CrossRef]
50. Holmberg, K. Surfactants. In *Ullmann's Encyclopedia of Industrial Chemistry*; Wiley Online Library: Hoboken, NJ, USA, 2019; pp. 1–56.
51. Li, H.; Qiu, Y. Dispersion, sedimentation and aggregation of multi-walled carbon nanotubes as affected by single and binary mixed surfactants. *R. Soc. Open Sci.* **2019**, *6*, 190241. [CrossRef]
52. Bai, Y.; Park, I.S.; Lee, S.J.; Bae, T.S.; Watari, F.; Uo, M.; Lee, M.H. Aqueous dispersion of surfactant-modified multiwalled carbon nanotubes and their application as an antibacterial agent. *Carbon* **2011**, *49*, 3663–3671. [CrossRef]
53. Upadhyayula, V.K.K.; Gadhamshetty, V. Appreciating the role of carbon nanotube composites in preventing biofouling and promoting biofilms on material surfaces in environmental engineering: A review. *Biotechnol. Adv.* **2010**, *28*, 802–816. [CrossRef]
54. Tan, Y.; Resasco, D.E. Dispersion of Single-Walled Carbon Nanotubes of Narrow Diameter Distribution. *J. Phys. Chem. B* **2005**, *109*, 14454–14460. [CrossRef]
55. Islam, M.F.; Rojas, E.; Bergey, D.M.; Johnson, A.T.; Yodh, A.G. High Weight Fraction Surfactant Solubilization of Single-Wall Carbon Nanotubes in Water. *Nano Lett.* **2003**, *3*, 269–273. [CrossRef]
56. Rastogi, R.; Kaushal, R.; Tripathi, S.K.; Sharma, A.L.; Kaur, I.; Bharadwaj, L.M. Comparative study of carbon nanotube dispersion using surfactants. *J. Colloid Interface Sci.* **2008**, *328*, 421–428. [CrossRef]
57. Bricha, M.; El Mabrouk, K. Effect of surfactants on the degree of dispersion of MWNTs in ethanol solvent. *Colloids Surf. A: Physicochem. Eng. Asp.* **2019**, *561*, 57–69. [CrossRef]
58. Goh, P.S.; Ng, B.C.; Ismail, A.F.; Aziz, M.; Sanip, S.M. Surfactant dispersed multi-walled carbon nanotube/polyetherimide nanocomposite membrane. *Solid State Sci.* **2010**, *12*, 2155–2162. [CrossRef]

59. Samanta, S.K.; Fritsch, M.; Scherf, U.; Gomulya, W.; Bisri, S.Z.; Loi, M.A. Conjugated Polymer-Assisted Dispersion of Single-Wall Carbon Nanotubes: The Power of Polymer Wrapping. *Acc. Chem. Res.* **2014**, *47*, 2446–2456. [CrossRef]
60. Gomulya, W.; Costanzo, G.D.; de Carvalho, E.J.F.; Bisri, S.Z.; Derenskyi, V.; Fritsch, M.; Fröhlich, N.; Allard, S.; Gordiichuk, P.; Herrmann, A.; et al. Semiconducting Single-Walled Carbon Nanotubes on Demand by Polymer Wrapping. *Adv. Mater.* **2013**, *25*, 2948–2956. [CrossRef]
61. Lassi, U.; Hu, T.; Pohjalainen, E.; Kallio, T.; Kordas, K.; Jantunen, H. Effect of a Surfactant Assisted Synthesis on the Electrochemical Performance of a LiFePO4-CNT Composite Electrode. *Int. J. Mater. Sci.* **2014**, *4*, 1–7. [CrossRef]
62. Wang, Z.; Jing, L.; Zheng, X.; Xu, Z.; Yuan, Y.; Liu, X.; Fu, A.; Guo, Y.-G.; Li, H. Microspheres of Si@Carbon-CNTs composites with a stable 3D interpenetrating structure applied in high-performance lithium-ion battery. *J. Colloid Interface Sci.* **2023**, *629*, 511–521. [CrossRef] [PubMed]
63. Li, X.; Jeong, Y.J.; Jang, J.; Lim, S.; Kim, S.H. The effect of surfactants on electrohydrodynamic jet printing and the performance of organic field-effect transistors. *Phys. Chem. Chem. Phys.* **2018**, *20*, 1210–1220. [CrossRef] [PubMed]